Molecular Biology of the Cell
Vol. 13, 3532–3545, October 2002

The Mammalian Septin MSF Localizes with Microtubules and Is Required for Completion of Cytokinesis

Mark C. Surka, Christopher W. Tsang, and William S. Trimble*

Programme in Cell Biology, Hospital for Sick Children and Department of Biochemistry, University of Toronto, Toronto, Ontario M5G 1X8, Canada

Submitted January 24, 2002; Revised June 14, 2002; Accepted August 5, 2002
Monitoring Editor: John Pringle

Cytokinesis in animal cells involves the contraction of an actomyosin ring formed at the cleavage furrow. Nuclear division, or karyokinesis, must be precisely timed to occur before cytokinesis in order to prevent genetic anomalies that would result in either cell death or uncontrolled cell division. The septin family of GTPase proteins has been shown to be important for cytokinesis although little is known about their role during this process. Here we investigate the distribution and function of the mammalian septin MSF. We show that during interphase, MSF colocalizes with actin, microtubules, and another mammalian septin, Nedd5, and coprecipitates with six septin proteins. In addition, transfections of various MSF isoforms reveal that MSF-A specifically localizes with microtubules and that this localization is disrupted by nocodazole treatment. Furthermore, MSF isoforms localize primarily with tubulin at the central spindle during mitosis, whereas Nedd5 is mainly associated with actin. Microinjection of affinity-purified anti-MSF antibodies into synchronized cells, or depletion of MSF by small interfering RNAs, results in the accumulation of binucleated cells and in cells that have arrested during cytokinesis. These results reveal that MSF is required for the completion of cytokinesis and suggest a role that is distinct from that of Nedd5.

INTRODUCTION

Cell division must be tightly regulated to ensure that daughter cells receive the appropriate complement of cellular and genetic material. Failure to divide correctly could lead to cell death or to alterations in genetic content that could cause unregulated cellular division and tumor growth. It has been shown that a family of GTPase proteins, called septins, is important for cell division in a wide range of organisms (Neufeld and Rubin, 1994; Longtine *et al.*, 1996; Kinoshita *et al.*, 1997). In the budding yeast *Saccharomyces cerevisiae*, temperature-sensitive mutations in any of four septins (Cdc3p, Cdc10p, Cdc11p, and Cdc12p) result in cells that fail to form the "neck filaments" beneath the cleavage furrow (Byers and Goetsch, 1976) and lead to multinucleated cells at the restrictive temperature (Hartwell, 1971). Biochemical studies have shown that the yeast septins assemble into a complex consisting of nearly equal amounts of Cdc3p, Cdc10p, Cdc11p, and Cdc12p (Frazier *et al.*, 1998), although the significance of their filamentous appearance remains unclear.

The function of septins during cytokinesis remains poorly understood. In *Drosophila*, a mutation in the septin gene *pnut* results in a lethal phenotype with multinucleated cells (Neufeld and Rubin, 1994), and Pnut and another *Drosophila* septin, Sep1, have been shown to colocalize with the contractile ring of dividing cells (Neufeld and Rubin, 1994; Fares *et al.*, 1995). As in yeast, the *Drosophila* septins Pnut, Sep1, and Sep2 copurify as a multimolecular complex in near stoichiometric ratios (Field *et al.*, 1996). However, some cell division events in *Drosophila* may not require the septins; for example, female germline stem cells can apparently divide without the involvement of Pnut or Sep1 (Adam *et al.*, 2000). In *Caenorhabditis elegans*, mutations in the septins UNC-59 and UNC-61 result in some postembryonic cell division defects, and immunofluorescence studies on wild-type organisms revealed colocalization at the leading edge of the cleavage furrow (Nguyen *et al.*, 2000). However, in this organism the septins are not required for embryonic cell division events. Finally, in dividing mammalian cells, the septin Nedd5 is localized to the cleavage furrow along with actin, and inhibitory antibody microinjections have suggested a role for Nedd5 in cytokinesis (Kinoshita *et al.*, 1997).

Article published online ahead of print. Mol. Biol. Cell 10.1091/mbc.E02–01–0042. Article and publication date are at www.molbiolcell.org/cgi/doi/10.1091/mbc.E02–01–0042.

* Corresponding author. E-mail address: wtrimble@sickkids.on.ca.

Abbreviations used: siRNA: small interfering RNA.

© 2002 by The American Society for Cell Biology

In addition to Nedd5, 10 other mammalian septin genes have been identified (reviewed in Kartmann and Roth, 2001), and for most of these little is known about their functions. However, expression analysis has revealed that many septins are expressed in nonmitotic tissues such as the brain, making it unlikely that they are exclusively involved in cytokinesis. In particular, CDCrel-1 was shown to play a role in exocytosis in secretory cells, possibly by binding directly to the SNARE protein syntaxin to regulate evoked secretion (Beites *et al.*, 1999). Septins were also implicated in secretion when they were copurified from the mammalian brain in association with the Sec6/8 complex that is thought to function in vesicle trafficking (Hsu *et al.*, 1998). In that study, several septins including Nedd5, CDC10, Septin 6, and H5 were purified in complexes similar to those previously characterized for yeast and *Drosophila*.

The *MSF* gene product, first identified in rat with the sec 6/8 complex (Hsu *et al.*, 1998), was originally named E-septin (Fung and Scheller, 1999), and two splice variants, long and short, were identified at that time. MSF orthologues have also been found in mice (Sorensen *et al.*, 2000) and humans (Osaka *et al.*, 1999), and in each of the species studied so far, its transcripts undergo complex splicing (Fung and Scheller, 1999; Osaka *et al.*, 1999; Taki *et al.*, 1999; Jackisch *et al.*, 2000; Kalikin *et al.*, 2000; Russell *et al.*, 2000; Sorensen *et al.*, 2000, 2002; McIlhatton *et al.*, 2001). *MSF*, *CDCrel-1*, and *KIAA0128/Septin 6* have all recently been shown to be fusion partners of the *MLL* protooncogene in cases of both de novo and therapy-related acute myeloid leukemia (Megonigal *et al.*, 1998; Osaka *et al.*, 1999; Taki *et al.*, 1999; Borkhardt *et al.*, 2001). This linkage has suggested the possibility of a role for MSF in tumorigenesis. In addition, the frequent deletion of *MSF* alleles in loss-of-heterozygosity studies of ovarian and breast tumors has led to the suggestion that MSF may play a role as a tumor suppressor (Kalikin *et al.*, 2000; Russell *et al.*, 2000).

To begin to understand the nature of the *MSF* gene with regards to tumorigenesis, we set out to characterize MSF protein function within the cells by determining its distribution and the effect of functional inhibition by antibody microinjection or depletion of endogenous MSF protein by use of small interfering RNA (siRNA). We show that unlike Nedd5, which associates with the cleavage furrow, MSF is associated with the mitotic spindle and is required for the completion of cytokinesis in mammalian cells.

MATERIALS AND METHODS

Cell Culture

HeLa cells were cultured in DMEM (Dulbecco's modified Eagle's medium) supplemented with 10% FBS and grown in a humidified incubator with 5% CO_2 at 37°C. Cells were synchronized at G1/S with a double aphidicolin block (1.25 μg/ml in DMEM overnight, followed by release for 9 h and treatment again overnight; Hamanaka *et al.*, 1995). HeLa cells typically entered M phase 9.5 h after the second aphidicolin release. For nocodazole treatment, nocodazole (Sigma-Aldrich, St. Louis, MO) was added to a final concentration of 10 μM in DMEM, and cells were grown as above for 30 min.

Plasmid Constructions and Transient Transfections

PCR products from normal human breast tissue cDNA corresponding to the coding region of MSF-A (nucleotides 10–1793, accession number AF189713) and MSF (nucleotides 776-2494, accession number NM_006640) were kindly provided in pCR-XL-TOPO (Invitrogen Corp., Carlsbad, CA) by E. Petty and L. Kalikin (University of Michigan, Ann Arbor). A GST fusion construct of MSF-A was constructed by subcloning the coding region of MSF-A from pCR-XL-TOPO (cut with *Hin*dIII and *Eco*RV) and blunt-end ligating into pGEX-KG (Guan and Dixon, 1991) digested with *Xba*I. A PCR product from a cDNA (Accession number T56977) encoding human CDC10 was subcloned into *Bam*HI-*Eco*RI–digested pGEX-KG (Pharmacia). All clones were confirmed by DNA sequencing. GST fusion constructs of mouse Nedd5 and human H5 were described previously (Xie *et al.*, 1999). GST fusion proteins were induced with 0.1 mM IPTG (Sigma-Aldrich) and purified on glutathione-agarose beads (Sigma-Aldrich) by affinity purification. Fusion proteins were electrophoresed on SDS-PAGE and Western blotted.

Myc-tagged MSF was constructed by subcloning pCR-XL-TOPO MSF digested with *Spe*I and *Eco*RV into pcDNA3.1 (Invitrogen Corp.) digested with *Eco*RV. Upstream of MSF, a myc epitope was inserted into the *Nhe*I site using the following oligonucleotides: 5′-CTAGAGCCACCATGGAGCAGAAGCTGATCAGCGAAGAGGACCTG-3′ and 5′-CTAGCAGGTCCTCTTCGCTGATCAGCTTCTGCTCCAT-3′. Myc-tagged MSF-A was constructed by digesting pCR-XL-TOPO MSF-A with *Hin*dIII and *Eco*RV, subcloning into *Hin*dIII-*Eco*RV–digested pcDNA3.1, and myc-tagging as above. Myc-tagged Nedd5 was constructed through digestion of pGEX-Nedd5 (Xie *et al.*, 1999) with *Bam*HI and *Eco*RI, ligating into *Bam*HI-*Eco*RI–digested pcDNA3.1, and myc tagging as above. All clones were confirmed by DNA sequencing. 0.5 μg of Myc-tagged vectors were transfected into HeLa cells grown on coverslips at 50% confluency using FuGene6 (Roche Applied Science, Indianapolis, IN) according to the manufacturer's directions. Protein expression was permitted for 12–16 h, and then the cells were processed for immunofluorescence as described below.

Anti-MSF Antibody Production

Peptide TDAAPKRVEIQVPKPC, corresponding to the N-terminal amino acids 4–18 of rat E-septin long form (accession number AAF01206), was synthesized and conjugated to KLH (Pierce Chemical, Rockford, IL) for immunization. Rabbit polyclonal antibodies were raised and subsequently purified on sulfolink beads (Pierce Chemical) to which the peptide was covalently attached. Anti-Nedd5 antibodies were described previously (Xie *et al.*, 1999). Anti-Septin 6 antibody was kindly provided by D. Roth and B. Kartmann.

Protein Extraction and Western Blotting

Rat tissues were homogenized in H-buffer (10 mM HEPES, pH 7.5, 150 mM NaCl, 300 mM sucrose) containing protease inhibitors (1 μg/ml pepstatin, 1 μg/ml leupeptin, 0.3 mM PMSF, 0.5 mM EDTA). Protein concentrations were measured by dot blot using BSA standards. The same volume of 2× Laemmli loading buffer (0.06 M Tris-HCl, pH 6.8, 2% SDS, 10% glycerol, 0.025% [wt/vol] bromophenol blue) was added to each crude tissue lysate, the sample was boiled and sonicated, and the insoluble material was spun down at 16 000 × *g* (Tabletop Centrifuge 5415D; Eppendorf, Hamburg, Germany). Approximately 20 μg of tissue, 10 μg soluble HeLa cell lysate (see Immunoprecipitations), or 25 ng of recombinant protein were electrophoresed on SDS PAGE and Western blotted.

Western blotting was performed as previously described (Gaisano *et al.*, 1994). Anti-MSF, anti-Nedd5, and anti–β-Actin (Sigma-Aldrich) were used at 1:1000 dilution, and anti–Septin 6 serum was used at 1:7000. To visualize protein bands, the blots were incubated with appropriate HRP-conjugated secondary antibodies (BIO-RAD Laboratories, Hercules, CA) for 1 h, washed extensively, and then incubated with chemiluminescence substrate (ECL; Amersham, Piscataway, NJ).

Immunofluorescence Microscopy

Cells were fixed with 2% paraformaldehyde in either phosphate-buffered saline (PBS) or microtubule-stabilization buffer (0.1 M MES, pH 6.9, 2 mM EGTA, 2 mM $MgCl_2$, 4% PEG 8000) for 20 min and subsequently processed as described previously (Xie *et al.*, 1999). Anti-MSF and anti-Nedd5 were used at 1:1000 dilution, monoclonal 9E3 myc antibody (Santa Cruz Biotechnology, Santa Cruz, CA) was used at 1:250 dilution, and monoclonal α-tubulin antibody (Sigma-Aldrich) was used at 1:2000. Goat anti-rabbit/mouse Cy3 (Jackson ImmunoResearch Laboratories, West Grove, PA) or Alexa Fluor 488 (Molecular Probes, Eugene, OR) conjugated secondary antibodies were used at a 1:2500 dilution. Actin staining was visualized with either rhodamine- or Oregon green–conjugated phalloidin (Molecular Probes). DAPI was used at 1 μg/ml in PBS for 5 min to stain nuclei. Coverslips were mounted on slides using DAKO fluorescent mounting medium (DAKO, Carpinteria, CA) and imaged using a Leica DM IRE2 (Deerfield, IL) inverted microscope furnished with a Hamamatsu ORCA ER (Malvern, PA) charge-coupled device camera. Cell images were captured using OpenLab v.3.0.7 (Improvision, Boston, MA) and analyzed using Adobe Photoshop 6.0 (San Jose, CA).

Fluorescent Conjugation of Anti-MSF and Anti-Nedd5 Antibodies

Anti-MSF and anti-Nedd5 crude sera were subjected to ammonium sulfate precipitation to enrich for IgG. Precipitated IgG was extensively dialyzed against PBS overnight. Approximately 60 mg of either anti-MSF or anti-Nedd5 IgG was incubated with 6-(tetramethylrhodamine-5-(and-6)-carboxamido)hexanoic acid, succinimidyl ester, or 6-(fluorescein-5-(and-6)-carboxamido)hexanoic acid, succinimidyl ester (Molecular Probes), respectively, in a 1:10 M ratio (protein:dye). Labeling was performed according to the manufacturer's directions with the unlabeled conjugate removed from the reaction by column chromatography over a PD-10 column (Amersham). Labeled antibody was then affinity-purified as described above. Fluorescently labeled antibodies were used for immunofluorescence, as described above, at concentrations ranging from 1:50 to 1:500.

Immunoprecipitations

HeLa cells were grown in 100-mm dishes to ~70% confluence before medium was removed, and the cells were washed once with ice-cold PBS, scraped in PBS with a rubber policeman, and collected. Cells were solubilized in HKA (10 mM HEPES, pH 7.5, 140 mM potassium acetate, 1 mM $MgCl_2$, 100 μM EGTA) buffer containing protease (1 μg/ml pepstatin, 2 μg/ml leupeptin, 2 mM PMSF) and phosphatase (50 mM NaF, 400 μM sodium orthovanadate) inhibitors and 1% Triton X-100. Cells were lysed by passing through a 27-gauge needle 3–5 times and rotated at 4°C for 30 min. Lysates were spun down at 100,000 × *g* for 10 min, and the soluble material was used for subsequent immunoprecipitations. Fractionation experiments have shown that this soluble fraction contains most, if not all, HeLa cell septins (unpublished observations).

Approximately 500 μg of solubilized HeLa cell lysate was used for each immunoprecipitation. Briefly, 3 μg of antibody was added to 40 μl of 50% protein-A agarose beads (Invitrogen) and rotated for 1 h at 4°C. The beads were washed three times with HKA buffer, and HeLa cell lysate was added along with NaCl to a final concentration of 150 mM. The mixtures were rotated at 4°C for 1–2 h and washed five times with RIPA buffer (1% Nonident P-40, 1% sodium deoxycholate, 0.1% SDS, 150 mM NaCl, 0.01 M sodium phosphate, pH 7.2, 2 mM EDTA) containing phosphatase inhibitors. The resultant pellets were resuspended in Laemmli loading buffer, containing 10 mM *N*-ethylmaleimide (Sigma-Aldrich) to help prevent the reduction of the IgG molecules and subjected to SDS-PAGE and Western blotting.

Protein Identification by MALDI-TOF-MS Analysis

HeLa cells were grown as above, and ~2 mg of solubilized HeLa cell lysate was used to precipitate the septin complex. Briefly, the immunoprecipitations were carried out exactly as described above using 12 μg of antibody added to 100 μl of 50% protein-A agarose beads. Pellets were resuspended in 1× NuPAGE LDS sample buffer (Invitrogen) containing 10 mM *N*-ethylmaleimide and boiled. Supernatants were subjected to electrophoresis on NuPAGE 4–12% Bis-Tris gradient gels (Invitrogen) according to the manufacturer's instructions and subsequently stained in Coomassie blue for 1 h, followed by destaining in 50% H_2O, 40% methanol, 10% acetic acid. Unknown protein bands were excised and subjected to in-gel trypsin digests (Shevchenko *et al.*, 1996) using modified trypsin (Promega, Madison, WI). Digestion and peptide elution was carried out as described previously (Figeys *et al.*, 2001), and eluted peptides were purified using PRP-3 resin (10 μm; Hamilton Company, Reno, NV). Briefly, 10 μl of 50% (wt/vol) PRP-3 resin (dissolved in 1:1 acetonitrile:H_2O) was added to the extracted peptide solution. The mixture was rotated at room temperature for 1 h and washed twice with 2% acetonitrile/1% acetic acid. Peptides were eluted by the addition of 15 μl 85% acetonitrile/1% acetic acid and subjected to MALDI-TOF-MS analysis.

The identity of MSF-A was confirmed by the presence of a tryptic peptide corresponding to the unique N-terminus of this isoform from two independent experiments. For the identification of human CDC10, 12 peptides matched the computed masses for the peptides from this septin (accession number AAB31337), which has a predicted mass of 49 kDa. The peptides covered 124 of 418 amino acids or 30% of the sequence.

Microinjections

HeLa cells grown on 25-mm coverslips were synchronized in G1/S as described above. Cells were microinjected 6 h after release using an Eppendorf Microinjector System (Eppendorf). Microinjections were carried out using anti-MSF antibodies or control rabbit IgG (Jackson ImmunoResearch Laboratories) antibodies at a concentration of 2 mg/ml and using an initial pressure of 250 hPa for 0.2 s. Cells were allowed to recover for 20 h before proceeding with immunofluorescence as described above but without incubation with primary antibody. Four (n = 4) and six (n = 6) independent experiments were performed using anti-MSF and rabbit IgG, respectively. Approximately 55 cells were microinjected in each individual experiment. Individual cells were injected at a spacing of at least 0.2 mm so as to be able to discriminate between a cell that has successfully divided and two individual cells.

siRNA Treatment

siRNA directed toward nucleotides 472–492, relative to the start codon of the MSF isoform MSF-B (GenBank accession number AF189712), and control siRNA directed toward CDCrel-1 were purchased from Dharmacon Research (Lafayette, CO) as double-stranded, desalted, and gel-purified preparations. The sequence used for siRNA was selected according to the guidelines from Elbashir *et al.* (2001), and the MSF siRNA should recognize all known human MSF mRNA species. Control siRNA was directed toward the rat septin isoform CDCrel-1 because HeLa cells do not express this septin (C.W.T. and W.S.T., unpublished observations). Transfection of siRNA using Lipofectamine 2000 (Invitrogen) was performed according to the manufacturer's directions. Briefly 240 pmol of siRNA was used to transfect ~100,000 HeLa cells grown in a single well of a six-well plate. Cells were grown on coverslips for

60 h and processed for immunofluorescence. Three and five independent experiments for control and MSF siRNA, respectively, were performed in which defects in cell division were scored using DAPI staining. Approximately 250 cells were counted in each experiment. In parallel experiments, transfected HeLa cells were treated with PBS plus 2 mM EDTA for 10 min and collected, and cells were counted and resuspended in Laemmli buffer for Western blot analysis to observe MSF protein levels. Approximately 15,000 cells were loaded in each lane, and actin was monitored as a loading control.

RESULTS

Expression Profile of MSF Proteins

To explore the properties of the *MSF* gene product, rabbit polyclonal antibodies were generated against an MSF peptide, and the specificity of these antibodies was tested on bacterially expressed GST-fusion proteins. As shown in Figure 1A, the anti-MSF antibodies recognized only MSF-A among several mammalian septin proteins. When used to probe Triton X-100–solubilized HeLa cell lysate, the anti-MSF antibodies identified three immunoreactive species (Figure 1B). Two have similar molecular weights of ~65 kDa, whereas the third migrated at ~55 kDa. Incubation of the antibody with the peptide to which it was raised eliminated this immunoreactivity, indicating that these three species were specifically detected by the antibody (Figure 1B). The specificity of the MSF antibody was also supported strongly by the immunoprecipitation experiments presented in Figure 2. The same set of bands was immunoprecipitated with anti-MSF and anti-Nedd5, including the three bands detected by anti-MSF; a cross-reactive species recognized by the MSF antibody would not be expected to precipitate with anti-Nedd5 (Figure 2, A–C).

The existence of additional MSF species in HeLa cells cannot be ruled out because our antibody would only recognize 12 of the 15 putative MSF isoforms recently described (McIlhatton *et al.*, 2001). Based on the approximate molecular weights of the three MSF bands, the upper two bands are likely to correspond to MSF-A, MSF, or Ovarian/Breast septin γ (or any of several splice variants that produce similar molecular weight species; McIlhatton *et al.*, 2001). The lower band is most consistent with MSF-B/C (Kalikin *et al.*, 2000; McIlhatton *et al.*, 2001).

Of the mammalian septin proteins studied to date, each has a unique tissue distribution (Caltagarone *et al.*, 1998; Yagi *et al.*, 1998; Beites *et al.*, 1999; Xie *et al.*, 1999; Zieger *et al.*, 2000), some being expressed primarily in the brain (CDCrel-1) and others being broadly expressed (Nedd5). To determine the tissue distribution of MSF, we probed a rat tissue Western and found that MSF-immunoreactive species were readily detectable in all tissues studied, except for skeletal muscle and intestine (Figure 1C). This correlates with, but is not identical to, the Northern blot of E-septin (the rat MSF orthologue; Fung and Scheller, 1999). Specifically, the Northern blot analysis revealed different hybridization patterns for testis and spleen, whereas the tissue western revealed identical protein banding patterns in these two tissues. This could indicate either that complex splicing of the MSF transcripts in these tissues produced similarly sized proteins or that there are MSF species present in these tissues that our antibody does not recognize. In addition, it remains possible that some of the species could represent degradation products, although these bands were consistently found in the specific tissues, and reprobing the blots for other proteins showed no evidence of degradation.

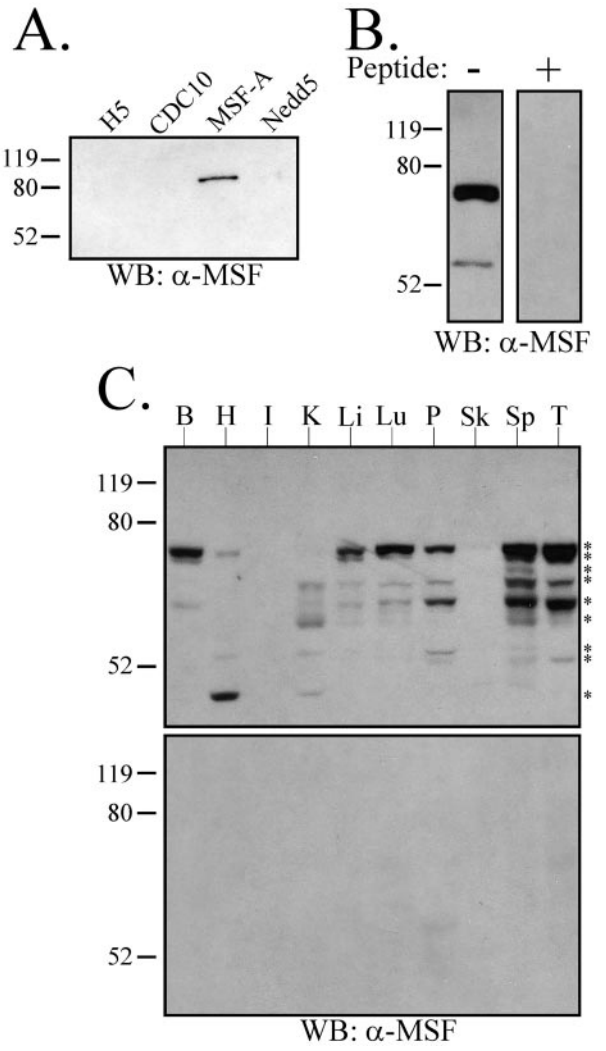

Figure 1. MSF immunoreactive species are found in HeLa cells and rat tissues. (A) The anti-MSF antibodies are specific for MSF septin. Approximately 25 ng of the indicated purified recombinant GST-septin proteins were electrophoresed and subjected to Western blotting using anti-MSF antibodies. (B) The anti-MSF antibodies recognize three immunoreactive species in HeLa cells. Ten micrograms of Triton X-100 HeLa cell lysate was electrophoresed, and a Western blot was performed in the absence (−) or presence (+) of the immunizing peptide. The upper two bands run as a close doublet that appears as a single band in this exposure (cf. Figure 2, A and B). (C) The anti-MSF antibodies recognize various species present in rat tissues. Twenty micrograms of whole tissue samples were electrophoresed, and a Western blot was performed in the absence (top blot) or presence (bottom blot) of the immunizing peptide. The following tissues were tested: B, Brain; H, Heart; I, Intestine; K, Kidney; Li, Liver; Lu, Lung; P, Pancreas; Sk, Skeletal Muscle; Sp, Spleen; T, Testis. Asterisks (*) denote nine individual immunoreactive species present in the tissues tested. Relative molecular weights in kDa are shown to the left of each blot.

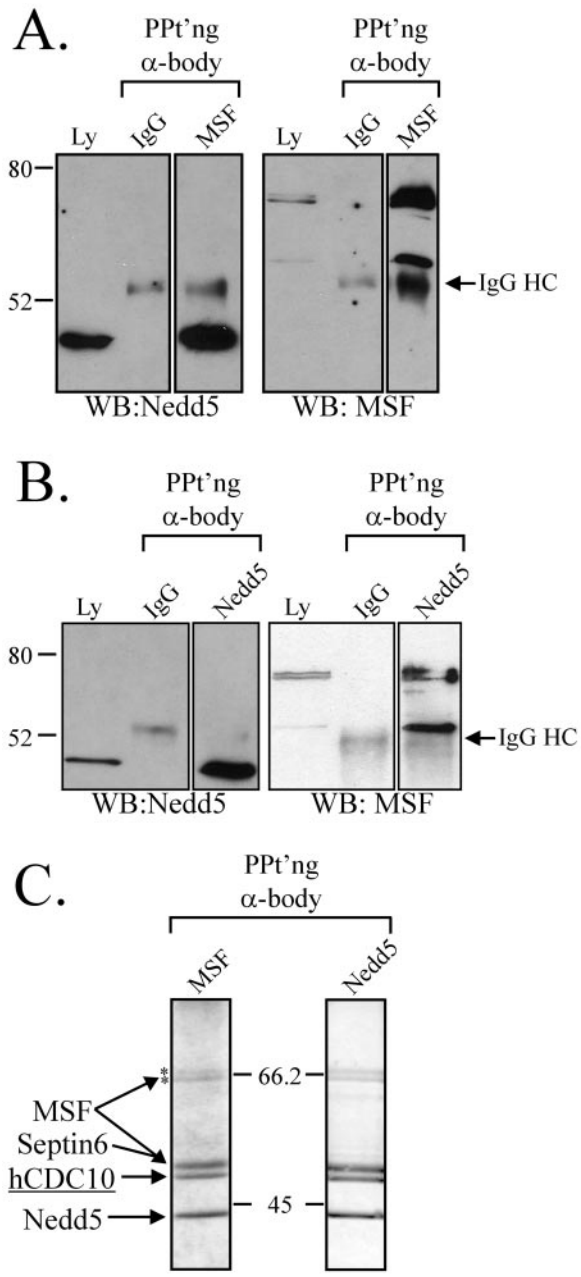

Figure 2. MSF and Nedd5 coimmunoprecipitate in a septin complex in interphase HeLa cells. Immunoprecipitations were performed as described in MATERIALS AND METHODS using anti-MSF (A and C) or anti-Nedd5 (B and C) antibodies and analyzed by Western blotting with the indicated antibodies (A and B) or by Coomassie blue staining (C). Samples of the starting material were also analyzed (Ly), and immunoprecipitations with nonimmune IgG provided a control. Western blots shown are representative of three independent experiments. Relative molecular weights and the position of the IgG heavy chain are indicated. In C, the identities of the protein bands were determined by Western blotting (A, B, and our unpublished results). hCDC10 was also identified by MALDI-TOF analysis of an in-gel trypsin digest of the protein band (see text). The NuPAGE 4–12% Bis-Tris gradient gels shown in C are representative of at least five independent experiments. Asterisks (*) denote the upper two MSF immunoreactive species.

Identification of Septin Complexes Present in HeLa Cells

Well-defined septin complexes can be isolated from both *Drosophila* and yeast. In mammalian cells, the large number of septin isoforms raises the possibility of much greater complexity in septin complex composition and therefore in function (Hsu *et al.*, 1998; Joberty *et al.*, 2001). To begin to address this issue, Nedd5 and MSF immunoprecipitations were performed using a soluble HeLa cell lysate. When Nedd5 was immunoprecipitated, all three immunoreactive species of MSF were coprecipitated, although the smallest form was enriched relative to its abundance in the lysate (Figure 2B). In the reciprocal experiment, Nedd5 coprecipitated with the three isoforms of MSF (Figure 2A).

Larger-scale immunoprecipitations were then performed as described in MATERIALS AND METHODS, and the resultant gels were stained with Coomassie blue. Six discrete bands were identified, with Nedd5 and MSF immunoprecipitations showing similar Coomassie staining patterns (Figure 2C). Four of the bands were identical in mobility to the bands detected by Western blotting for Nedd5 and the three forms of MSF. In addition, MALDI-TOF analysis of the upper two bands confirmed their identities as MSF isoforms (see MATERIALS AND METHODS), further supporting the specificity of the antibody. The upper band was demonstrated to contain peptides specific to MSF-A, whereas the lower band could not be specified but is most consistent in size with the isoform called MSF. A fifth septin band present on these gels was identified as Septin 6/KIAA0128 through Western blotting. The sixth band, with an apparent molecular weight of 50 kDa, was excised and subjected to tryptic digestion followed by MALDI-TOF analysis and was identified as the human septin protein CDC10 (accession number AAB31337; see MATERIAL AND METHODS). Interestingly, Nedd5, CDC10, and Septin 6 appeared to be roughly equivalent in staining intensity (Figure 2C), whereas the three MSF bands were significantly weaker. Hence, MSF isoforms associate with Nedd5, Septin 6, and CDC10 in HeLa cells. Although these may be individual interactions with MSF, their stoichiometry in both immunoprecipitations suggests that they represent a single complex of proteins.

MSF Colocalizes with Nedd5, Actin-based Filaments, and Microtubules in Interphase Cells

Previous studies have shown that Nedd5, CDC10, and Septin 6 colocalize in MDCK cells (Joberty *et al.*, 2001), and our immunoprecipitation data argued that Nedd5 and MSF should colocalize in HeLa cells. To test this, myc-tagged Nedd5 was transiently expressed in HeLa cells and the localization of myc-Nedd5 and endogenous MSF was assayed by immunofluorescence. In all the cells expressing low levels of myc-Nedd5, colocalization of the anti-myc and anti-MSF immunostaining was observed (Figure 3).

Previous studies of the mammalian septins Nedd5 and H5 have shown that both proteins are present near the plasma membrane and appear filamentous, colocalizing with the actin cytoskeleton (Kinoshita *et al.*, 1997; Xie *et al.*, 1999). The "filamentous" appearance of MSF colocalizing with Nedd5 prompted us to ask whether MSF colocalizes with actin. To investigate this, HeLa cells were double-stained using anti-MSF antibodies and phalloidin. As can be seen in Figure 4,

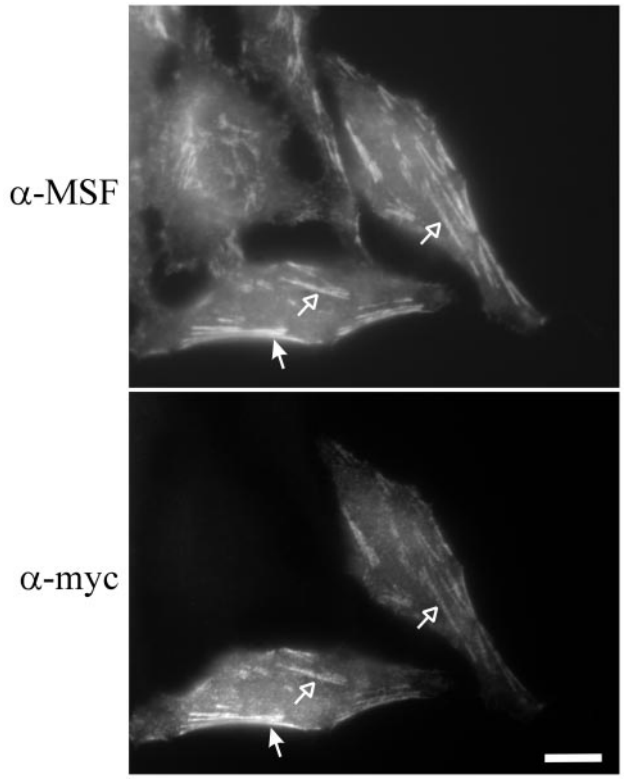

Figure 3. In interphase HeLa cells, MSF and Nedd5 colocalize along filaments, both within the central region of cells (open arrows) and along the periphery (filled arrows). Cells were transiently transfected with myc-tagged Nedd5 vector for 12 h, fixed, and subjected to anti-MSF (top) and anti-myc (bottom) immunostaining. Bar, 10 μm.

A–C, MSF appeared to colocalize with the central part of actin stress fibers (filled arrows), but was excluded from the focal adhesions (open arrows). In addition, in ~30% of stained cells when the focal plane of the microscope was raised toward the top of the cell, MSF staining also appeared as curvilinear structures around the nucleus (Figure 4D, open arrow) and projecting out toward the cell periphery (Figure 4D, closed arrows). This staining pattern is reminiscent of that of microtubules, and indeed MSF and α-tubulin appeared to colocalize (Figure 4, D–F). Fixation of cells with paraformaldehyde either in PBS or a microtubule stabilization buffer (see MATERIALS AND METHODS) gave similar immunostaining patterns; however, methanol fixation disrupted the colocalization of MSF with microtubules. Similar results were obtained using CHO cells, and the immunostaining of MSF was specific, because addition of the peptide used to generate the antibodies completely abolished the immunofluorescence. Myc-tagged rat isoforms of MSF (E-septin long and short) were previously shown to localize to membranes, with the short isoform localizing to tubular and vesicular structures along with perinuclear staining (Fung and Scheller, 1999). That study did not investigate possible colocalization with actin or microtubules; however, it appears that under the conditions used, the myc-tagged rat MSF isoforms did not appear filamentous.

MSF-A Localizes Specifically with the Microtubule Network

Previous studies on Nedd5 and H5 have shown that the "filamentous" septins are dependent on the actin cytoskeleton, because disruption of actin by cytochalasin D or latrunculin B abolishes the filamentous appearance of either septin (Kinoshita *et al.*, 1997; Xie *et al.*, 1999). The partial colocalization of MSF with tubulin prompted us to investigate the dependence of the curvilinear MSF structures on microtubules. Nocodazole was used to disrupt microtubules, and subsequent MSF, actin, and tubulin immunostaining was performed (Figure 5, A and B). When the microtubule network was disrupted, the MSF immunostaining pattern was now solely localized with the actin cytoskeleton (Figure 5A). Curvilinear filaments normally seen at higher focal planes were absent (Figure 5B). Washout of nocodazole allowed for the reformation of the MSF curvilinear structures.

From our MALDI-TOF analysis above, one specific MSF isoform present in HeLa cells is MSF-A. In addition, based on molecular-weight predictions, it appeared likely that another form present in HeLa cells is MSF. We therefore created myc-tagged MSF-A and MSF constructs. In all cells expressing low levels of myc-MSF, all the myc immunostaining appeared filamentous (Figure 5C) and colocalized with actin. Cells expressing myc-MSF-A revealed the presence of curvilinear structures, similar to the endogenous microtubule associated filaments (Figure 5E) and colocalized with tubulin. On microtubule disruption by nocodazole, the myc immunostaining pattern of myc-MSF remained filamentous (Figure 5D). In contrast, nocodazole disrupted the myc-MSF-A curvilinear pattern, which now appeared actin-like (Figure 5F), with no curvilinear structures present even at higher focal planes (Figure 5F, inset). Collectively, the myc-MSF and myc-MSF-A staining patterns revealed the full complement of endogenous MSF immunostaining as seen with our antibodies.

Differential Localization of MSF and Nedd5 during Cell Division

During cell division, the septins localize to the division site in both yeast and animal cells (see INTRODUCTION). In mammalian cells, the filamentous appearance of the septins Nedd5 and H5 disappears at the onset of mitosis, and during cytokinesis they localize to the cleavage furrow along with actin (Kinoshita *et al.*, 1997; Xie *et al.*, 1999). It seemed plausible that all mammalian septins would behave similarly; however, immunofluorescence analysis of the distribution of MSF during cell division revealed a different pattern.

During metaphase to early telophase, MSF exhibited a punctate staining pattern with concentrations of immunoreactivity between the separating chromosomes (Figures 6A and 7, A and C, Metaphase to Early Telophase, open arrows) and at the distal ends of the cells (Figures 6A and 7, A and C, Metaphase to Early Telophase, filled arrows). During telophase, when the cleavage furrow begins to constrict, MSF did not colocalize with actin at the cleavage furrow but was present where there is a gap in the actin staining of the cleavage furrow (Figure 6A, Telophase to Late Telophase, open arrows and asterisk). Indeed, MSF concentrated with tubulin until the formation of the midbody (Figure 7A, Early

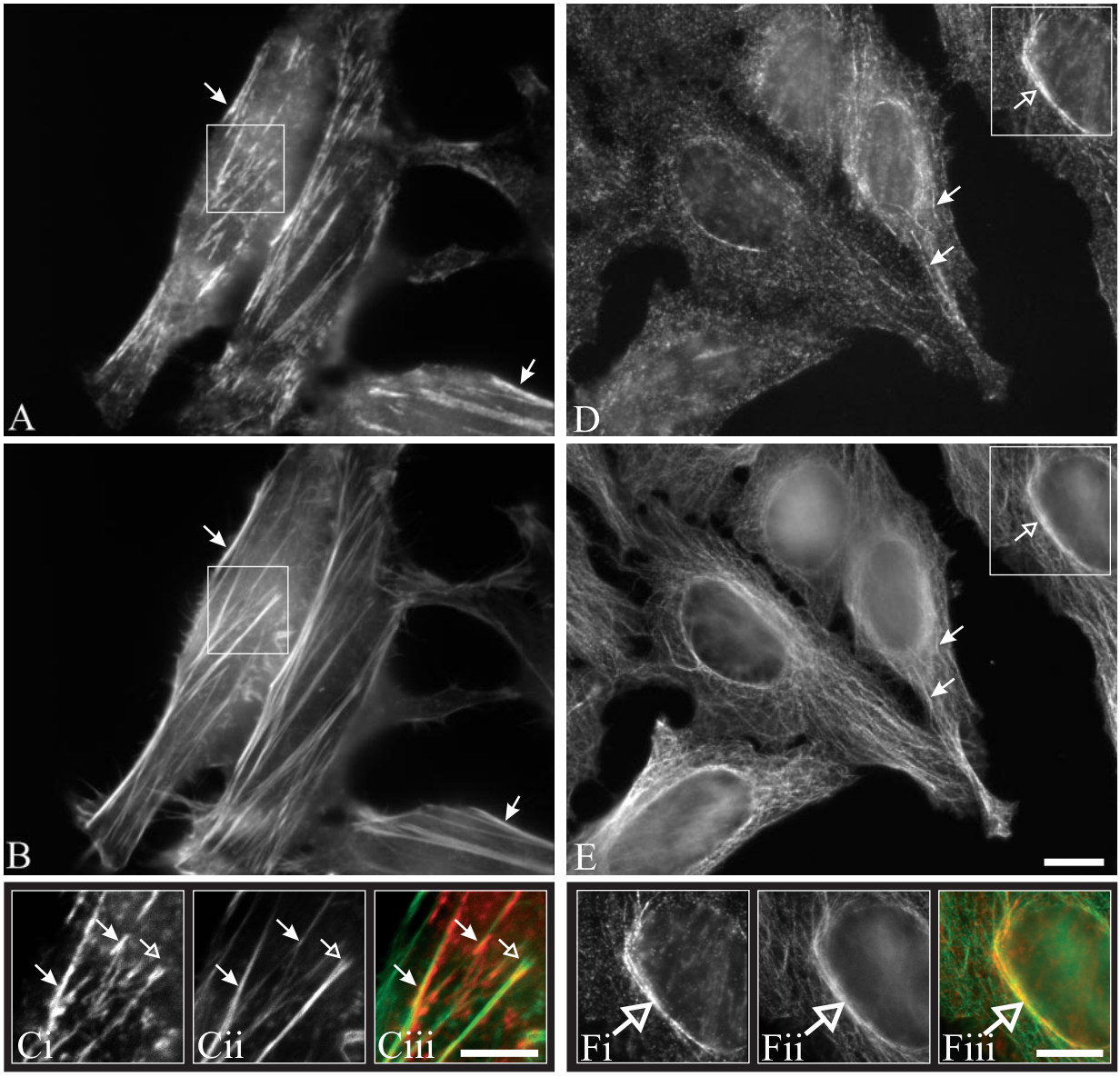

Figure 4. MSF is found along actin stress fibers and microtubules. HeLa cells grown on coverslips were prepared for immunofluorescence as described in MATERIALS AND METHODS. Cells were double-labeled either with anti-MSF antibodies (A) and phalloidin (B) or with anti-MSF antibodies (D) and monoclonal α-tubulin antibodies (E). To detect actin-MSF colocalization, focus was set near the bottom of the cell, whereas MSF-tubulin colocalization was seen at higher focal planes. (C and F) Enlarged images of the boxed regions. MSF immunostaining (Ci and Fi); actin (Cii) or tubulin (Fii); and, overlays (Ciii and Fiii) with MSF staining in red, and actin (Ciii) or tubulin (Fiii) staining in green. Arrows indicate features discussed in the text. Bar, 10 μm (A–F).

to Late Telophase, open arrows). During this stage, Nedd5 colocalized primarily with actin at the cleavage furrow (Figure 6B, Telophase to Late Telophase, filled arrows) but eventually did reveal some concentration with tubulin and MSF at the central spindle (Figure 7, B and C, Late Telophase, open arrows). Of 24 cells captured at this stage in Nedd5/MSF double-labeling experiments, only 11 of the cells showed colocalization of MSF and Nedd5 on the central spindle, and these appeared to have highly constricted midzones typical of late telophase. These differences in localization suggest that Nedd5 and MSF may have different functions during cytokinesis (see DISCUSSION).

Interference with MSF Function Disrupts Cell Division in HeLa Cells

To date, only one mammalian septin has been shown to play a role in cytokinesis, by experiments in which microinjection of anti-Nedd5 antibodies into late anaphase/early telophase HeLa cells interfered with cytokinesis (Kinoshita *et al.*, 1997).

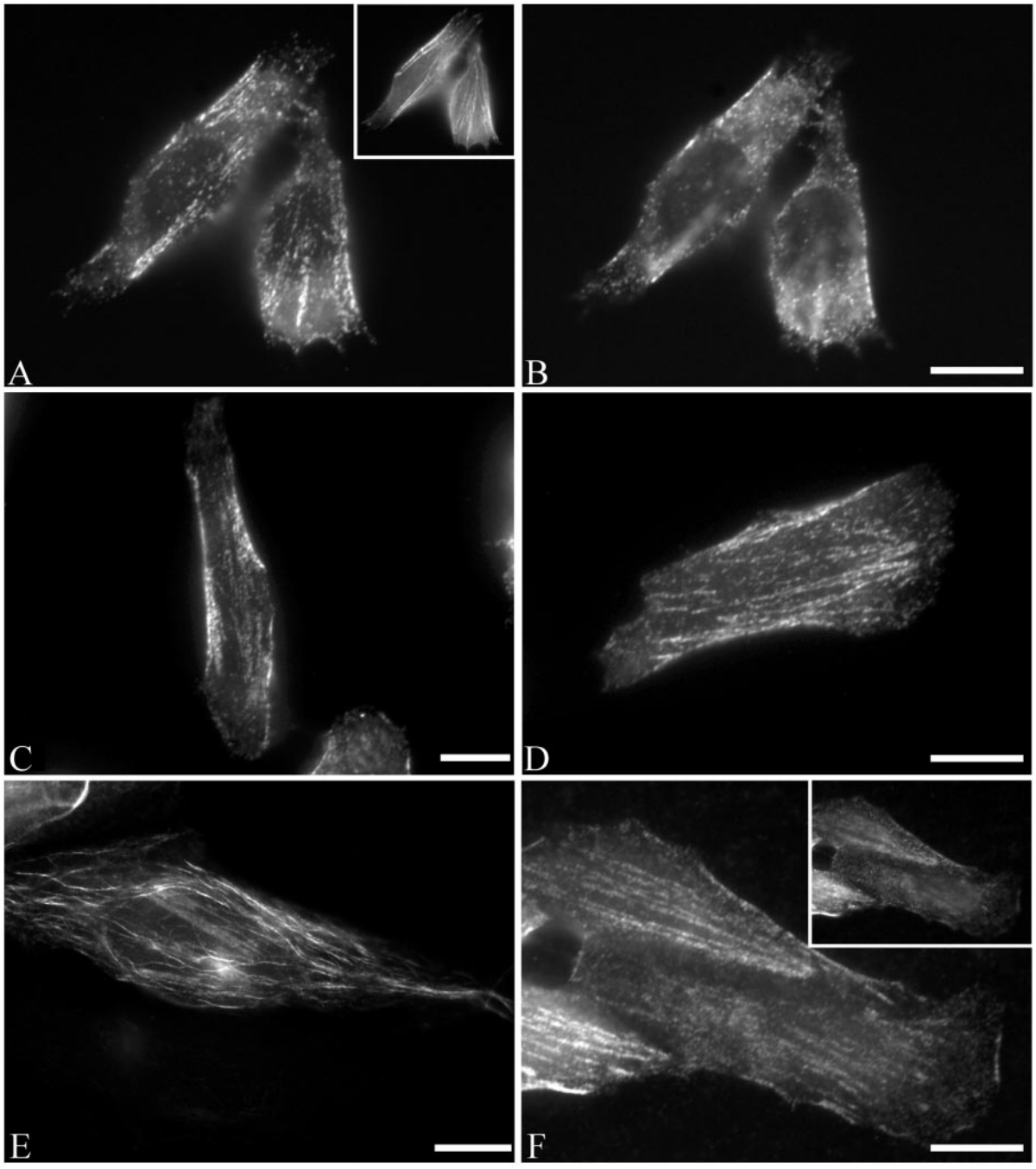

Figure 5. MSF-A localizes specifically with tubulin and is disrupted by nocodazole. (A and B) Endogenous MSF is partially sensitive to nocodazole. HeLa cells grown on coverslips were treated with 10 μM nocodazole and prepared for immunofluorescence. Cells were double-labeled with anti-MSF antibodies (A and B) and phalloidin (inset, A) and photographed with a focus either near the plane of cell attachment (A) or higher in the cell (B) where tubulin-associated MSF would normally be seen (cf. Figure 4). Tubulin-associated MSF curvilinear filaments were disrupted by nocodazole while actin-associated MSF was unaffected. Raising the focus off the plane of cell-attachment did not reveal the presence of any curvilinear structures (B). (C and D) HeLa cells were transiently transfected with the myc-tagged MSF vector without (C) or with (D) 10 μM nocodazole for 30 min, fixed, and subjected to anti-myc immunostaining. (C) myc MSF localizes to actin-like structures. (D) Nocodazole treatment had no effect on the pattern of mycMSF. (E and F) HeLa cells were transfected with the myc-tagged MSF-A vector without (E) or with (F) nocodazole treatment as in D. Curvilinear filaments were seen above the plane of cell attachment in mycMSF-A transfected cells (E), but these became linear like actin-associated filaments after nocodazole treatment (F; photographed near the plane of cell attachment). Raising the plane of focus still did not reveal the appearance of any curvilinear structures in the nocodazole-treated cells (F, inset). Bars, 10 μm.

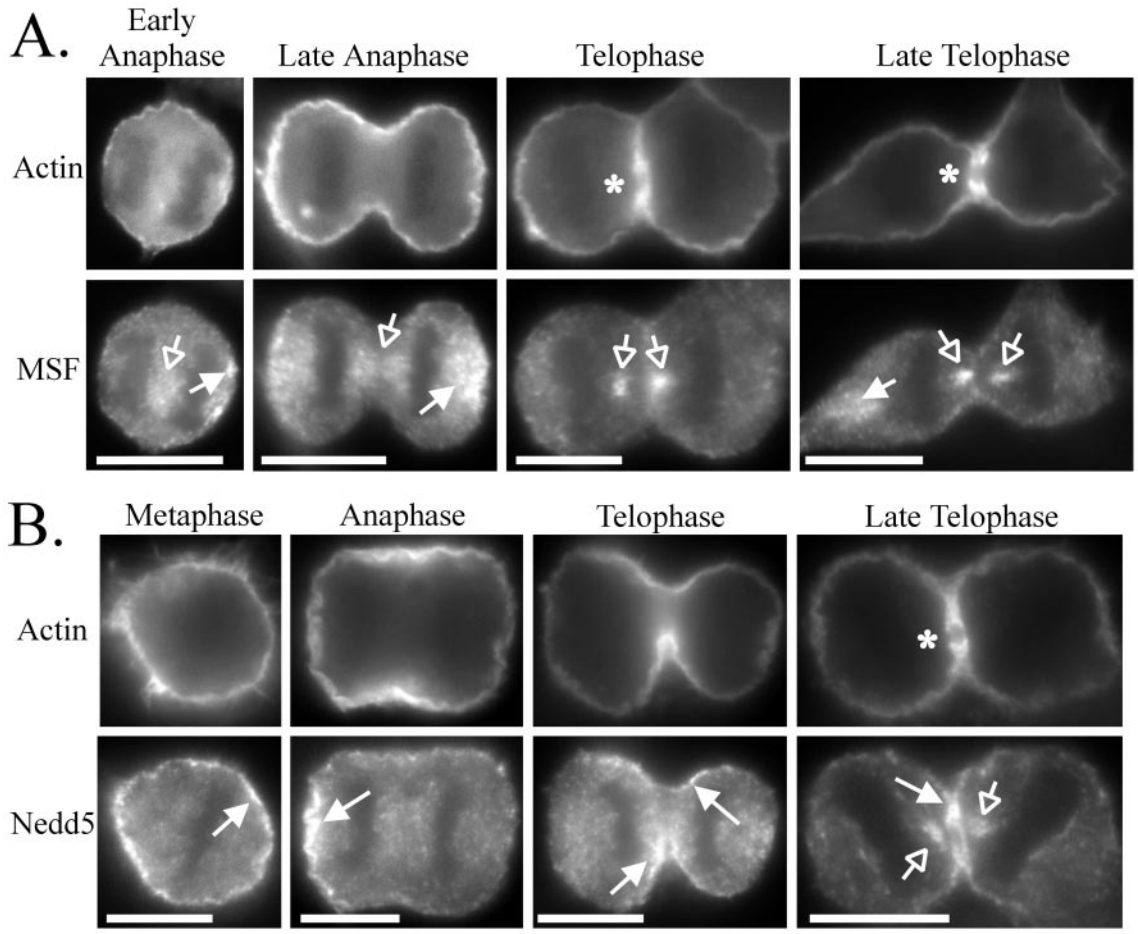

Figure 6. Differential localization of MSF and Nedd5 relative to actin during cell division. HeLa cells were fixed on coverslips, permeabilized, and double-stained for actin and either MSF (A) or Nedd5 (B). DAPI staining was used to assay the phase during cell division. Arrows and asterisks indicate features discussed in the text. Bars, 10 μm.

To determine if MSF is also required for cell division, MSF-specific antibodies were injected into synchronized HeLa cells ~4 h before division. The injected cells were then allowed to recover overnight before examination in order to permit the resolution of intermediate effects that might not be apparent at earlier time points. A total number of 215 and 325 cells were microinjected with anti-MSF and nonspecific IgG, respectively, with ~60–80% of microinjected cells positive for antibody the next day (see MATERIALS AND METHODS). No apparent morphological defects (other than those described below) were noted in either anti-MSF– or rabbit IgG-injected cells. However, when anti-MSF–injected cells were compared with IgG-injected cells, it was evident that injection of MSF antibodies frequently caused defects in cell division (Figure 8A). A total of 45 microinjected cells were defective in cell division out of 155 positive cells for MSF antibody, whereas only a total of 7 microinjected cells were defective out of 211 positive cells for control rabbit IgG. On closer examination of the anti-MSF–injected cells that had failed to complete cell division, several phenotypes were observed. Approximately 65% of these cells contained two nuclei (Figure 8B), indicating that cytokinesis had failed. In addition, two other phenotypes were observed. Eleven percent of the cells had one daughter cell with abnormal morphology and condensed DNA, reminiscent of apoptosis, and 24% of the cells remained attached with daughter cells connected by a short midbody bridge. Within most of these midbodies (8/11), DAPI-positive structures resembling DNA appeared trapped in this region. Of the cells injected with rabbit IgG that displayed defects in cell division (Figure 8A), five contained double nuclei and two were arrested at the midbody stage. Neither of these two contained DNA within their midbodies, and they appeared rounded, unlike the flat morphology seen within anti-MSF–positive cells.

Previous work using siRNA in cultured mammalian cells has shown this technique to be efficient at reducing protein levels in a specific manner (Elbashir *et al.*, 2001a, 2001b; Harborth *et al.*, 2001). Therefore, double-stranded siRNA was synthesized corresponding to the MSF coding region that would theoretically recognize all MSF mRNA splice variants present in HeLa cells. Control (see MATERIALS AND METHODS) and MSF siRNA were transfected into cells grown on coverslips and allowed to grow for 60 h. Defects in cell division were scored by DAPI staining and, as

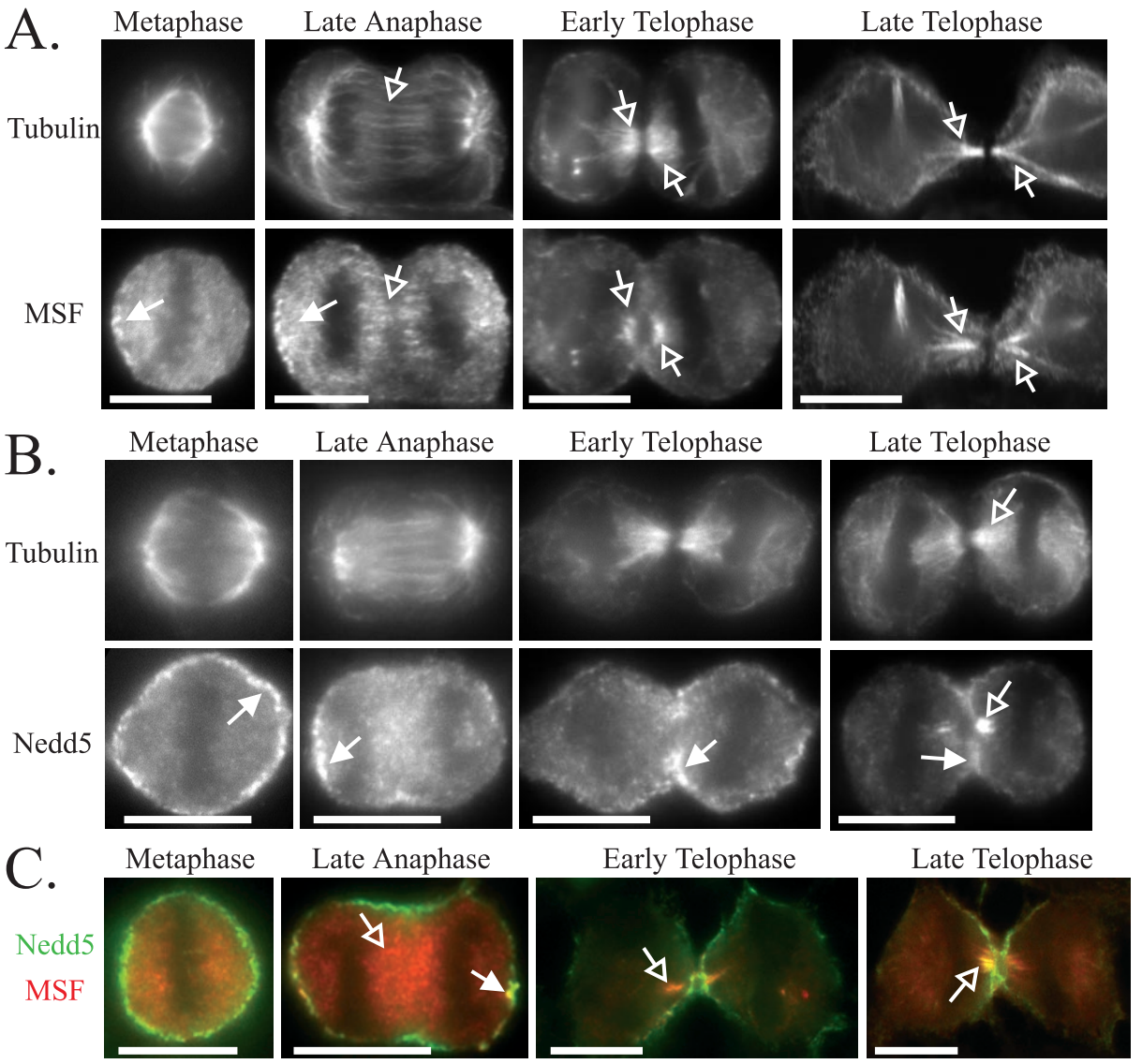

Figure 7. Differential localization of MSF and Nedd5 relative to tubulin, and each other, during cell division. HeLa cells were fixed on coverslips, permeabilized, and double-stained for tubulin and MSF (A), tubulin and Nedd5 (B), or MSF and Nedd5 (C). The double-staining in C used fluorophore-conjugated primary antibodies (see MATERIALS AND METHODS). DAPI staining was used to assay the phase of cell division. Arrows indicate features discussed in the text. Bars, 10 μm.

can be seen in Figure 8C, MSF siRNA-treated cells displayed failed cell division much more frequently than did control siRNA-treated cells. A total of 1239 MSF siRNA-treated cells were counted, with a total of 264 cells that failed cell division. In the control experiments, a total of 675 cells were counted, with only 7 cells failing to divide. MSF immunostaining was decreased in MSF siRNA-treated cells compared with control cells and, by Western blot analysis, MSF protein levels were reduced between 60 and 80% as determined by densitometric scans (Figure 8D). Fewer cells were detected in the MSF siRNA-treated cells than in control treated cells, suggesting that slowed growth or increased cell death resulted from MSF reduction. It is noteworthy that the percentage of cells displaying defective divisions is similar for both antibody microinjection (Figure 8A) and siRNA (Figure 8C) methods.

DISCUSSION

In this study we characterized the distribution and function of the mammalian septin MSF. Antibodies specific for the N-terminus of the rat orthologue of MSF-B/C (rat E-septin long), which are specific for the MSF septins, recognize three MSF isoforms present in HeLa cells (Figure 1, A and B). In a variety of rat tissues, this antibody recognized at least nine immunoreactive species (Figure 1C), supporting previous studies indicating that transcripts from the *MSF* gene un-

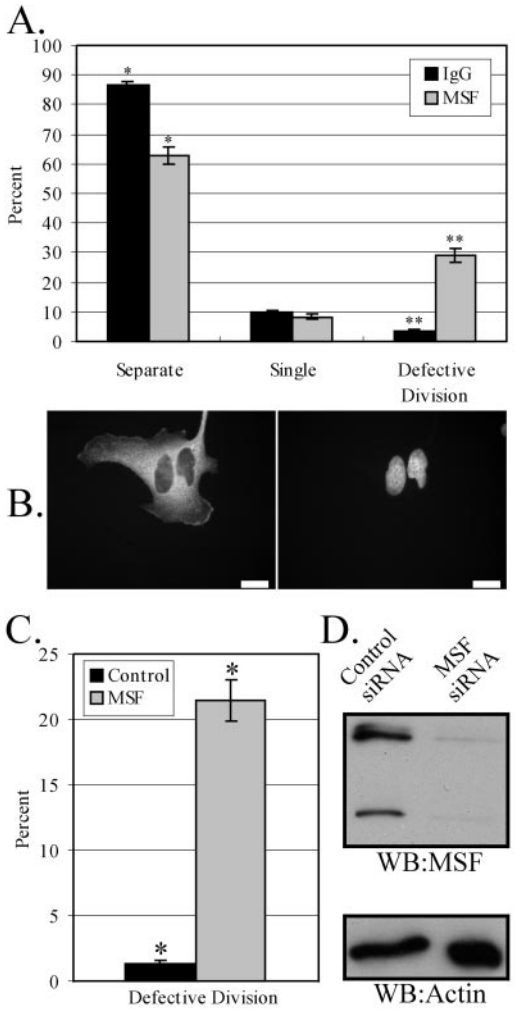

Figure 8. tk;3Both microinjection of anti-MSF antibodies and reduction of MSF by siRNA cause defects in cell division. (A) Quantification of control (IgG) or anti-MSF injected phenotypes. Cells were synchronized on coverslips in S phase (MATERIALS AND METHODS) and microinjected 6 h after release. Cells were allowed to recover for 20 h, and phenotypes were assayed by immunofluorescence using Cy3-conjugated anti-rabbit IgG antibodies and DAPI staining. "Separate" represents injected cells that have successfully undergone division; "Single" represents injected cells that are alone; and "Defective Division" represents cells that have a failure in cytokinesis (see text). Data are expressed as mean ± SEM; *$p < 0.02$, Student's *t* test; **$p < 0.01$, Student's *t* test, significantly different. (B) Immunofluorescence image of a typical double-nucleus phenotype observed, indicating failure in cell division. Left: immunocytochemical detection of injected antibody; right: the DAPI staining. Bars, 10 μm. (C) Quantification of defective division in control (*CDCrel-1*) or *MSF* siRNA-transfected HeLa cells. Cells were grown on coverslips and transfected with siRNA (MATERIALS AND METHODS), and phenotypes were assayed by DAPI staining. "Defective Division" is counted as in A. Data are expressed as mean ± SEM; *$p < 0.0002$, Student's *t* test, significantly different. (D) Western blot revealing a decrease in MSF protein levels in siRNA-treated cells compared with the control cells. Equal numbers of cells were loaded per lane and probed with anti-MSF antibodies (top panel) or anti–β-actin antibodies (bottom panel) as a loading control. Western blotting results are representative of two independent experiments.

dergo complex splicing (Osaka *et al.*, 1999; Taki *et al.*, 1999; Jackisch *et al.*, 2000; Kalikin *et al.*, 2000; Russell *et al.*, 2000; McIlhatton *et al.*, 2001; Sorensen *et al.*, 2002). Indeed, a recent study showed that there may be as many as 18 different splice variants of human MSF mRNA, encoding at least 15 different MSF proteins (McIlhatton *et al.*, 2001). To date, four rat and four mouse MSF isoforms have been described; however, it appears from our data that additional isoforms may also exist in these organisms.

MSF colocalizes with actin, microtubules, and another mammalian septin, Nedd5, in interphase cells (Figures 3 and 4). These two septins were shown to coimmunoprecipitate from the detergent-soluble cell lysate of interphase cells. When the MSF and Nedd5 immunoprecipitations were analyzed by Coomassie blue staining, at least six individual proteins were found to coprecipitate (Figure 2C). Through Western blot and MALDI-TOF mass spectrometry analyses, these bands were identified as the three MSF immunoreactive species, Nedd5, hCDC10, and Septin 6/KIAA0128. This analysis further complements the recent data indicating that Nedd5, hCDC10, Septin 6/KIAA0128, and one of the upper MSF species copurify on a GST-BORG column from NIH 3T3 cell lysates (Joberty *et al.*, 2001). Whether or not these individual septins associate into one multimolecular complex or if these data reflect the presence of a mixture of smaller septin complexes is currently under investigation. However, similar coprecipitation patterns with both Nedd5 and MSF antibodies argue in favor of a single septin complex. The exact stoichiometries and complete protein composition of mammalian septin complexes present in different cell types remain to be determined.

Support for the notion that septins may form specific types of complexes has been described in other systems. In yeast there exist two sporulation-specific septins (Ozsarac *et al.*, 1995; De Virgilio *et al.*, 1996), and it has been hypothesized that different septin complexes may be acting in vegetative and sporulating cells (reviewed in Field and Kellogg, 1999). In *Drosophila*, the septins Pnut, Sep1, and Sep2 colocalize at sites of embryo cellularization (Neufeld and Rubin, 1994; Adam *et al.*, 2000); however, in *Pnut* null embryos, Sep2 localizes normally despite the absence of Sep1, revealing a possible hierarchy of septin arrangement or assembly into different septin complexes under these conditions (Adam *et al.*, 2000). In addition, in mammals, it has been noted that different septins are present in different tissues and even different cell types within a particular tissue (Hsu *et al.*, 1998; Beites *et al.*, 1999; Xie *et al.*, 1999; Kinoshita *et al.*, 2000; this study). The differential expression of septins within a particular cell or tissue type may govern the septin complex(es) that can be formed and its associated functions.

In interphase HeLa cells, MSF antibodies detected two types of filamentous patterns. Near the bottom of the attached cells, MSF immunoreactivity colocalized with Nedd5 and actin stress fibers. In the middle of the cell, MSF immunoreactivity appeared more curvilinear and colocalized with tubulin filaments. Interestingly, transfection of myc-tagged MSF-A isoform mimicked the tubulin-associated pattern, whereas transfection of the myc-MSF isoform mimicked the actin-associated pattern. Hence, the anti-MSF antibody reflected the sum of the distributions observed for the different isoforms. Moreover, the MSF-A isoform is identical to MSF except for the first 20 amino acids, which are distinct from

the first 7 of MSF (Kalikin *et al.*, 2000). This strongly suggests that a microtubule association domain is likely to be present within this region of MSF-A.

In contrast to interphase cells, during cell division Nedd5 and MSF show little colocalization and may have distinct roles in this process (Figures 6 and 7). The MSF immunoreactivity did not concentrate at the cleavage furrow (Figures 6A and 7, A and C), as has been seen for other septins such as Nedd5 (Kinoshita *et al.*, 1997; and this study) and H5 (Xie *et al.*, 1999). Instead, MSF concentrated along with tubulin between the separating chromosomes and at the central spindle (Figure 7, A and C). This region is devoid of actin, suggesting that MSF localization during cell division is not actin dependent. Colocalization between MSF and tubulin at the central spindle during cytokinesis, and specific disruption of the MSF-tubulin colocalization by nocodazole in interphase cells, raises the possibility of a relationship between MSF and microtubule organization during cytokinesis.

In our microinjection and siRNA transfection experiments, we have shown that MSF is important and perhaps required for cell division. Antibody microinjections may interfere with the function of the protein either by directly inhibiting it or by indirectly affecting protein function by steric hindrance. In any case, microinjection of anti-MSF antibody resulted in several phenotypes in addition to the binucleated cells often seen when cytokinesis fails. It had been shown previously that disruption of septin function produces multinucleated cells in yeast (Hartwell, 1971; Longtine *et al.*, 1996), *Drosophila* (Neufeld and Rubin, 1994), *C. elegans* (Nguyen *et al.*, 2000), and mammals (Kinoshita *et al.*, 1997). However, we also observed phenotypes indicating improper or arrested cytokinesis, in which cells appeared to have attempted fission but failed. This is consistent with several studies that have shown that the central spindle is required for the completion of cytokinesis (Wheatley and Wang, 1996; Canman *et al.*, 2000). Interestingly, recent studies have shown that movement of the centrosome to the midbody region is essential to complete the abscission process, and failure to do so results in bridged cells with elongated midbodies (Piel *et al.*, 2001). The observations that some anti–MSF-injected cells had DNA trapped within their midbody and had gone through improper cytokinesis suggests that anti-MSF injection may disrupt karyokinesis or cause premature cytokinesis. The incomplete inhibition of cytokinesis may reflect redundancy for MSF function or may indicate that the cells have completed division by unconventional means. Indeed, the bridges that connect these cells were often extremely long, suggestive of cells that had migrated apart in an effort to divide despite this connection, similar to the "attachment-assisted" mitotic cleavage (Neujahr *et al.*, 1997; Uyeda *et al.*, 2000) that *Dictyostelium discoideum* are capable of when cleavage furrow function is blocked.

Reduction of MSF protein levels by siRNA techniques also resulted in defects in cytokinesis, albeit with less pleotropic phenotypes. The lack of similar phenotypes as those seen in the microinjection experiments could be due to the time difference between the two approaches. The siRNA-treated cells are allowed to grow for 2.5 d posttransfection, and within this time period, defects such as those listed above may occur but avoid observation because cell death also occurs. Indeed, there was an approximately twofold decrease in the total number of cells present after MSF siRNA treatment compared with the control. Whether or not this reduction is due to a lag in the cell cycle, an increase in cell death, or a combination of the two, is currently under investigation.

The *MSF* gene has previously been implicated in a number of mammalian cancers, including acute myeloid leukemia (Osaka *et al.*, 1999; Taki *et al.*, 1999), T-cell lymphomas (Sorensen *et al.*, 2000), and ovarian and breast tumors (Kalikin *et al.*, 2000; Russell *et al.*, 2000). In the leukemias, the *MLL* gene was found to be fused in-frame with the *MSF* gene (Osaka *et al.*, 1999; Taki *et al.*, 1999), whereas in breast and ovarian tumors a region of chromosome 17q25 including the *MSF* gene was found to undergo loss-of-heterozygosity (Russell *et al.*, 2000). Together, these observations could suggest that MSF may act as a tumor suppressor gene and that its loss of function could be important in malignancy. However, our data suggesting that MSF is required for cell division do not fit well with a role as a tumor suppressor. Alternatively, abrogation of MSF function may lead to aberrant cytokinesis events that could contribute to tumor progression. In any case, colocalization of MSF with tubulin during cytokinesis suggests that its role in this process may be unexpectedly different from that of other septins. Future studies will be aimed at determining the precise role of MSF in mitosis.

ACKNOWLEDGMENTS

We thank Drs. E. Petty and L. Kalikin for generously providing MSF cDNA clones used in this study and Drs. D. Roth and B. Kartmann for anti-Septin 6 antibody. M.C.S. and C.W.T. hold Doctoral Awards from, and W.S.T. is an Investigator of, the Canadian Institutes for Health Research. This work was funded by a grant from the National Cancer Institute of Canada with funds from the Canadian Cancer Society.

REFERENCES

Adam, J.C., Pringle, J.R., and Peifer, M. (2000). Evidence for functional differentiation among *Drosophila* septins in cytokinesis and cellularization. Mol. Biol. Cell *11*, 3123–3135.

Beites, C.L., Xie, H., Bowser, R., and Trimble, W.S. (1999). The septin CDCrel-1 binds syntaxin and inhibits exocytosis. Nat. Neurosci. *2*, 434–439.

Borkhardt, A., Teigler-Schlegel, A., Fuchs, U., Keller, C., Konig, M., Harbott, J., and Haas, O.A. (2001). An ins(X;11)(q24;q23) fuses the *MLL* and the *Septin 6/KIAA0128* gene in an infant with AML-M2. Genes Chromosomes Cancer *32*, 82–88.

Byers, B., and Goetsch, L. (1976). A highly ordered ring of membrane-associated filaments in budding yeast. J. Cell Biol. *69*, 717–721.

Caltagarone, J., Rhodes, J., Honer, W.G., and Bowser, R. (1998). Localization of a novel septin protein, hCDCrel-1, in neurons of human brain. Neuroreport *9*, 2907–2912.

Canman, J.C., Hoffman, D.B., and Salmon, E.D. (2000). The role of pre- and post-anaphase microtubules in the cytokinesis phase of the cell cycle. Curr. Biol. *10*, 611–614.

De Virgilio, C., DeMarini, D.J., and Pringle, J.R. (1996). *SPR28*, a sixth member of the septin gene family in *Saccharomyces cerevisiae*

that is expressed specifically in sporulating cells. Microbiology *142*, 2897–2905.

Elbashir, S.M., Harborth, J., Lendeckel, W., Yalcin, A., Weber, K., and Tuschl, T. (2001a). Duplexes of 21-nucleotide RNAs mediate RNA interference in cultured mammalian cells. Nature *411*, 494–498.

Elbashir, S.M., Lendeckel, W., and Tuschl, T. (2001b). RNA interference is mediated by 21- and 22-nucleotide RNAs. Genes Dev. *15*, 188–200.

Fares, H., Peifer, M., and Pringle, J.R. (1995). Localization and possible functions of *Drosophila* septins. Mol. Biol. Cell *6*, 1843–1859.

Field, C.M., al-Awar, O., Rosenblatt, J., Wong, M.L., Alberts, B., and Mitchison, T.J. (1996). A purified *Drosophila* septin complex forms filaments and exhibits GTPase activity. J. Cell Biol. *133*, 605–616.

Field, C.M., and Kellogg, D. (1999). Septins: cytoskeletal polymers or signaling GTPases? Trends Cell Biol. *9*, 387–394.

Figeys, D., McBroom, L.D., and Moran, M.F. (2001). Mass spectrometry for the study of protein-protein interactions. Methods *24*, 230–239.

Frazier, J.A., Wong, M.L., Longtine, M.S., Pringle, J.R., Mann, M., Mitchison, T.J., and Field, C. (1998). Polymerization of purified yeast septins: evidence that organized filament arrays may not be required for septin function. J. Cell Biol. *143*, 737–749.

Fung, E.T., and Scheller, R.H. (1999). Identification of a novel alternatively spliced septin. FEBS Lett. *451*, 203–208.

Gaisano, H.Y., Sheu, L., Foskett, J.K., and Trimble, W.S. (1994). Tetanus toxin light chain cleaves a vesicle-associated membrane protein (VAMP) isoform 2 in rat pancreatic zymogen granules and inhibits enzyme secretion. J. Biol. Chem. *269*, 17062–17066.

Guan, K.L., and Dixon, J.E. (1991). Eukaryotic proteins expressed in *Escherichia coli*: an improved thrombin cleavage and purification procedure of fusion proteins with glutathione *S*-transferase. Anal. Biochem. *192*, 262–267.

Hamanaka, R., Smith, M.R., O'Connor, P.M., Maloid, S., Mihalic, K., Spivak, J.L., Longo, D.L., and Ferris, D.K. (1995). Polo-like kinase is a cell cycle-regulated kinase activated during mitosis. J. Biol. Chem. *270*, 21086–21091.

Harborth, J., Elbashir, S.M., Bechert, K., Tuschl, T., and Weber, K. (2001). Identification of essential genes in cultured mammalian cells using small interfering RNAs. J. Cell Sci. *114*, 4557–4565.

Hartwell, L.H. (1971). Genetic control of the cell division cycle in yeast. IV. Genes controlling bud emergence and cytokinesis. Exp. Cell Res. *69*, 265–276.

Hsu, S.C., Hazuka, C.D., Roth, R., Foletti, D.L., Heuser, J., and Scheller, R.H. (1998). Subunit composition, protein interactions, and structures of the mammalian brain sec6/8 complex and septin filaments. Neuron *20*, 1111–1122.

Jackisch, B.O., Hausser, H., Schaefer, L., Kappler, J., Muller, H.W., and Kresse, H. (2000). Alternative exon usage of rat septins. Biochem. Biophys. Res. Commun. *275*, 180–188.

Joberty, G., Perlungher, R.R., Sheffield, P.J., Kinoshita, M., Noda, M., Haystead, T., and Macara, I.G. (2001). Borg proteins control septin organization and are negatively regulated by Cdc42. Nat. Cell Biol. *3*, 861–866.

Kalikin, L.M., Sims, H.L., and Petty, E.M. (2000). Genomic and expression analyses of alternatively spliced transcripts of the *MLL* septin-like fusion gene (*MSF*) that map to a 17q25 region of loss in breast and ovarian tumors. Genomics *63*, 165–172.

Kartmann, B., and Roth, D. (2001). Novel roles for mammalian septins: from vesicle trafficking to oncogenesis. J. Cell Sci. *114*, 839–844.

Kinoshita, A., Noda, M., and Kinoshita, M. (2000). Differential localization of septins in the mouse brain. J. Comp. Neurol. *428*, 223–239.

Kinoshita, M., Kumar, S., Mizoguchi, A., Ide, C., Kinoshita, A., Haraguchi, T., Hiraoka, Y., and Noda, M. (1997). Nedd5, a mammalian septin, is a novel cytoskeletal component interacting with actin-based structures. Genes Dev. *11*, 1535–1547.

Longtine, M.S., DeMarini, D.J., Valencik, M.L., Al-Awar, O.S., Fares, H., De Virgilio, C., and Pringle, J.R. (1996). The septins: roles in cytokinesis and other processes. Curr. Opin. Cell Biol. *8*, 106–119.

McIlhatton, M.A., Burrows, J.F., Donaghy, P.G., Chanduloy, S., Johnston, P.G., and Russell, S.E.H. (2001). Genomic organization, complex splicing pattern and expression of a human septin gene on chromosome 17q25.3. Oncogene *20*, 5930–5939.

Megonigal, M.D. *et al.* (1998). t(11;22)(q23;q11.2) in acute myeloid leukemia of infant twins fuses *MLL* with *hCDCrel*, a cell division cycle gene in the genomic region of deletion in DiGeorge and velocardiofacial syndromes. Proc. Natl. Acad. Sci. USA *95*, 6413–6418.

Neufeld, T.P., and Rubin, G.M. (1994). The *Drosophila* peanut gene is required for cytokinesis and encodes a protein similar to yeast putative bud neck filament proteins. Cell *77*, 371–379.

Neujahr, R., Heizer, C., and Gerisch, G. (1997). Myosin II-independent processes in mitotic cells of *Dictyostelium discoideum*: redistribution of the nuclei, re-arrangement of the actin system and formation of the cleavage furrow. J. Cell Sci. *110*, 123–137.

Nguyen, T.Q., Sawa, H., Okano, H., and White, J.G. (2000). The *C. elegans* septin genes, *unc-59* and *unc-61*, are required for normal postembryonic cytokinesis and morphogenesis but have no essential function in embryogenesis. J. Cell Sci. *113 Pt 21*, 3825–3837.

Osaka, M., Rowley, J.D., and Zeleznik-Le, N.J. (1999). *MSF* (MLL septin-like fusion), a fusion partner gene of *MLL*, in a therapy-related acute myeloid leukemia with a t(11;17)(q23;q25). Proc. Natl. Acad. Sci. USA *96*, 6428–6433.

Ozsarac, N., Bhattacharyya, M., Dawes, I.W., and Clancy, M.J. (1995). The *SPR3* gene encodes a sporulation-specific homologue of the yeast *CDC3/10/11/12* family of bud neck microfilaments and is regulated by ABFI. Gene *164*, 157–162.

Piel, M., Nordberg, J., Euteneuer, U., and Bornens, M. (2001). Centrosome-dependent exit of cytokinesis in animal cells. Science *291*, 1550–1553.

Russell, S.E. *et al.* (2000). Isolation and mapping of a human septin gene to a region on chromosome 17q, commonly deleted in sporadic epithelial ovarian tumors. Cancer Res. *60*, 4729–4734.

Shevchenko, A., Jensen, O.N., Podtelejnikov, A.V., Sagliocco, F., Wilm, M., Vorm, O., Mortensen, P., Boucherie, H., and Mann, M. (1996). Linking genome and proteome by mass spectrometry: large-scale identification of yeast proteins from two dimensional gels. Proc. Natl. Acad. Sci. USA *93*, 14440–14445.

Sorensen, A.B., Lund, A.H., Ethelberg, S., Copeland, N.G., Jenkins, N.A., and Pedersen, F.S. (2000). *Sint1*, a common integration site in SL3–3-induced T-cell lymphomas, harbors a putative proto-oncogene with homology to the septin gene family. J. Virol. *74*, 2161–2168.

Sorensen, A.B., Warming, S., Fuchtbauer, E.M., and Pedersen, F.S. (2002). Alternative splicing, expression, and gene structure of the septin-like putative proto-oncogene Sint1. Gene *285*, 79–89.

Taki, T., Ohnishi, H., Shinohara, K., Sako, M., Bessho, F., Yanagisawa, M., and Hayashi, Y. (1999). *AF17q25*, a putative septin family gene, fuses the *MLL* gene in acute myeloid leukemia with t(11;17)(q23;q25). Cancer Res. *59*, 4261–4265.

Uyeda, T.Q., Kitayama, C., and Yumura, S. (2000). Myosin II-independent cytokinesis in *Dictyostelium*. its mechanism and implications. Cell. Struct. Funct. *25*, 1–10.

Wheatley, S.P., and Wang, Y. (1996). Midzone microtubule bundles are continuously required for cytokinesis in cultured epithelial cells. J. Cell Biol. *135*, 981–989.

Xie, H., Surka, M., Howard, J., and Trimble, W.S. (1999). Characterization of the mammalian septin H5: distinct patterns of cytoskeletal and membrane association from other septin proteins. Cell Motil. Cytoskelet. *43*, 52–62.

Yagi, M., Zieger, B., Roth, G.J., and Ware, J. (1998). Structure and expression of the human septin gene. HCDCREL-1. Gene *212*, 229–236.

Zieger, B., Tran, H., Hainmann, I., Wunderle, D., Zgaga-Griesz, A., Blaser, S., and Ware, J. (2000). Characterization and expression analysis of two human septin genes, *PNUTL1* and. PNUTL2. Gene *261*, 197–203.